J. Anat. (1989), **166**, pp. 85–95
With 9 figures
Printed in Great Britain

Effects of atrial natriuretic peptide on Type II alveolar epithelial cells of the rat lung. Autoradiographic and morphometric studies*

YUKIO ISHII†, TSUYOSHI WATANABE, MASAHIKO WATANABE, SHIZUO HASEGAWA‡ AND YASUO UCHIYAMA

Departments of †Respiratory Internal Medicine and Anatomy, Institutes of ‡Clinical Medicine and Basic Medical Sciences, University of Tsukuba, Tsukuba, Ibaraki, Japan

(*Accepted* 7 *February* 1989)

INTRODUCTION

Type II alveolar epithelial (Type II) cells are known to produce pulmonary surfactant which reduces surface tension at the air–water interface (Goerke, 1974). The synthesis and/or secretion of surfactant material in Type II cells are facilitated by stimuli of neurohumoral mediators: cholinergic and adrenergic stimuli (Goldenberg, Buckingham & Sommers, 1969; Oyarzun & Clements, 1978; DeCamara, Moss & Das Gupta, 1979; Dobbs & Mason, 1979). It is well established that hormonal stimuli such as adrenal glucocorticoids and thyroid hormones accelerate differentiation of Type II cells and synthesis of surfactant (Farrell & Avery, 1975; Wu *et al.* 1973).

Atrial natriuretic peptides (ANP) stored in atrial myoendocrine cells of the heart (Cantin *et al.* 1984; Metz, Mutt & Forssmann, 1984) possess various biological actions: diuresis, natriuresis, vasodilatation and inhibition of aldosterone and cortisol hypersecretion (De Bold, Borenstein, Veress & Sonnenberg, 1981; Seidah *et al.* 1984; Garcia, Thibault, Cantin & Genest, 1984; De Lean *et al.* 1984). As far as the circulatory system is concerned, blood containing newly secreted ANP passes first through the lung tissue. This suggests the possibility that the lung tissue is a target organ of ANP. In fact, it has been confirmed that the lung tissue contains many binding sites for ANP (Bianchi *et al.* 1985) and ANP receptor can be purified from bovine lung (Ishido *et al.* 1986; Shimonaka *et al.* 1987).

During an autoradiographic study of the lung tissue using [^{125}I]ANP, we found silver grains over Type II cells in addition to endothelial cells and smooth muscle cells of vessels. In the present study, therefore, we analysed the effects of ANP on subcellular structures of Type II cells in the rat lung, using a morphometric technique.

MATERIALS AND METHODS

Preparation of [^{125}*I*]*ANP*

[^{125}I]ANP (Na^{125}I, 1 mCi/10 μl, Amersham) was prepared using synthetic rat α-ANP (α-rANP, Peninsula Laboratories Inc) with minor modifications of the Chloramine T method (Greenwood & Hunter, 1963). Immediately after reaction, the radioactive mixtures were separated on a Sep-Pak C18 cartridge column (Waters

* Reprint requests to Yasuo Uchiyama, Department of Anatomy, Institute of Basic Medical Sciences, University of Tsukuba, Tsukuba, Ibaraki-Ken 305, Japan.

Associates). Then the mixtures were applied to reverse phase HPLC, where three radioactive major peaks were obtained. Monoiodinated α-rANP, eluted in the second peak, was purified and used as a tracer which was stored at −80 °C until use. The siliconised glass tubes used for the storage of the tracer were treated with 1% bovine serum albumin (Sigma).

Injection of [^{125}I]ANP

[^{125}I]ANP (10 μCi; 12 ng) in 0·2 ml physiological saline was injected into the inferior vena cava of male, 50 g Wistar rats under sodium pentobarbitone anaesthesia. For displacement analysis, 6 μg α-rANP was mixed with [^{125}I]ANP as above and injected in the same manner.

Autoradiography

At 2 minutes after [^{125}I]ANP injection, 8 rats were perfused via the heart, first with the physiological saline for exactly 1 minute and then with 2% glutaraldehyde–2% paraformaldehyde buffered with 0·1 M cacodylate-HCl, pH 7·2, for 10 minutes. Portions of lung, kidney and liver tissues from each rat were used to quantitate radioactivity in a gamma counter (Beckman Gamma 4000). The lung tissue was cut into small pieces and further fixed with the same fixative for 2 hours. For light microscopy, samples were dehydrated with graded alcohols and embedded in JB-4. Sections were cut at 2 μm with an LKB ultramicrotome (2088 IV) and mounted on gelatin-coated glass slides. They were stained with haematoxylin and eosin or left unstained before dipping in Sakura NR-M2 emulsion. For electron microscopy, samples were postfixed with 2% OsO_4 buffered with 0·1 M cacodylate-HCl, pH 7·2, containing 7·5% sucrose for 2 hours. Then they were dehydrated with graded alcohols and embedded in Epon 812. Thin sections were cut with the ultramicrotome and mounted on Formvar-coated glass slides. They were stained with uranyl acetate and lead citrate and coated with carbon before dipping in Sakura NR-H2. All sections for light and electron microscopy were exposed for 4 weeks and developed by Konidol X (Sakura, Japan) for 5 minutes at 20 °C. Thin sections were then mounted on nickel grids and stained for 20 minutes with lead citrate before examination with a Hitachi H-600 electron microscope.

Procedures for α-rANP injection and electron microscopy

Nine μg α-rANP in 0·5 ml physiological saline were injected intraperitoneally into 8 male Wistar rats (12 weeks of age, *ca.* 250 g), respectively. At 5, 15, 30 and 60 minutes after the injection, 2 rats were perfused, first with 50 ml physiological saline and then with 250 ml of 2% glutaraldehyde–2% paraformaldehyde buffered with 0·1 M cacodylate-HCl, pH 7·2. Two rats killed at 0 minute in the same manner as above were not treated with ANP and were used as controls. The lung tissue was quickly excised from the middle lobe of the right lung, cut into small pieces (2 × 2 × 2 mm) and placed in the same fixative at 0 °C for 24 hours. After washing thoroughly with the same buffer containing 7·5% sucrose, the blocks were postfixed with 2% OsO_4 buffered with 0·1 M cacodylate-HCl, pH 7·2, containing 7·5% sucrose for 2 hours, and stained with 2% aqueous solution of uranyl acetate for 1 hour. The blocks were then dehydrated using graded alcohols and embedded in Epon 812. Silver sections were cut with an LKB ultramicrotome, and after staining with uranyl acetate and lead citrate, they were examined with the electron microscope.

The original magnification of electron micrographs was ×2210, calibrated using a

carbon grating replica with 2000 lines per mm. Eighteen fields of Type II cells from each rat were chosen randomly and photographed at the same magnification. Four to six Epon blocks were used for each rat.

Morphometry

The morphometric method used has been previously reported (Watanabe & Uchiyama, 1988). Various morphometric parameters of subcellular structures were measured: the volume, surface and numerical densities of lamellar bodies, the volume and surface densities of rough endoplasmic reticulum (RER), Golgi complex, multivesicular bodies and mitochondria in the cytoplasm of Type II cells. Measurement of surface densities of mitochondria was limited to their outer membranes.

The volume densities of various cytoplasmic organelles (Vv) and the numerical profile densities (N_A) were analysed at 10 times the original magnification by a universal projector (Olympus), using a double lattice system with 1·5 cm spacing (test points: 220). For the estimation of surface densities, the number of intersection points of cytoplasmic membranes with the test line was counted on the same screen of the instrument at the same magnifications.

The profile size of lamellar bodies was measured by an image-analysing system (nac Cardias GP-2000) at 10 times the original magnification. From the size distribution of lamellar bodies, the mean diameters (D) were calculated (Giger & Riedwyl, 1970). The Nv of lamellar bodies was calculated from the equation: $Nv = N_A/D$. The individual volume (V) of lamellar bodies was calculated by the equation: $V = Vv/Nv$.

The fractional values of each component at each sampling time were calculated for each electron micrograph (18 electron micrographs per rat, 36 electron micrographs per sampling time). The mean, standard deviation (S.D.) and standard error of the mean (S.E.) were obtained from all fractional values calculated at each sampling time. For the statistical evaluation, analysis of variance was applied to examine differences in morphometric parameters between the groups, using Tukey's comparison test.

Corrections of systemic errors occurring in the volume, surface and numerical densities of various components were performed after the method of Weibel (1979).

RESULTS

Autoradiography

The injection of an excess of ANP together with [^{125}I]ANP showed a significant inhibition of uptake of radioactive ANP; inhibition rates were 86·6% in the lung, 73·8% in the kidney and 65·3% in the liver (n = 4 for each).

Silver grains of [^{125}I]ANP were deposited over Type II cells, endothelial cells and smooth muscle cell layers of vessels, bronchi and bronchioles (Fig. 1*a,b,c*). In the controls, very few grains were detected in the lung tissue examined. With electron microscopy, silver grains were seen on the basal plasma membrane of Type II cells (Fig. 2).

The incidence of silver grains deposited on each constituent in the alveolar region of the lung tissue was calculated; endothelial cells were 29·4 ± 1·3% (± S.E.) and Type II cells 10·8 ± 1·2% (± S.E.). The numbers of silver grains per unit volume of each constituent in the alveolar tissue were 3·0 ± 0·4 (± S.E.) in endothelial cells and 3·9 ± 0·6 (± S.E.) in Type II cells (Fig. 3).

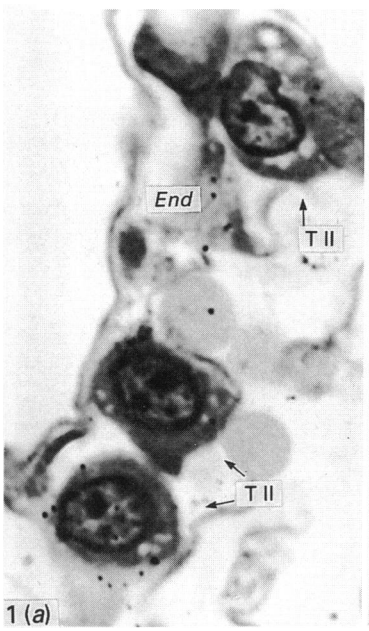

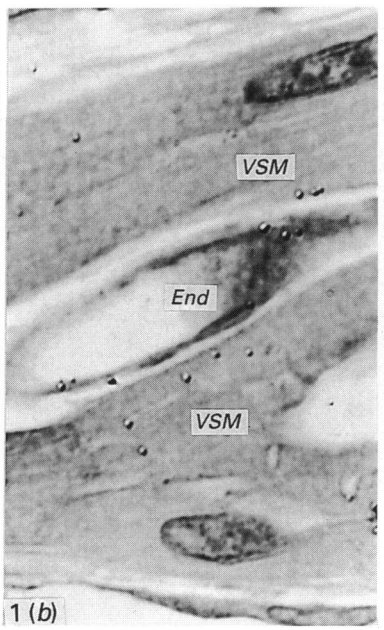

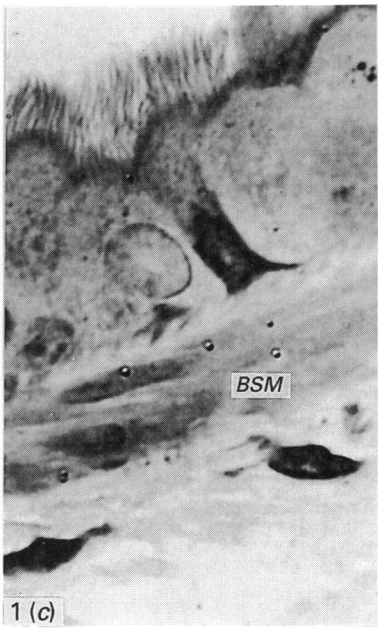

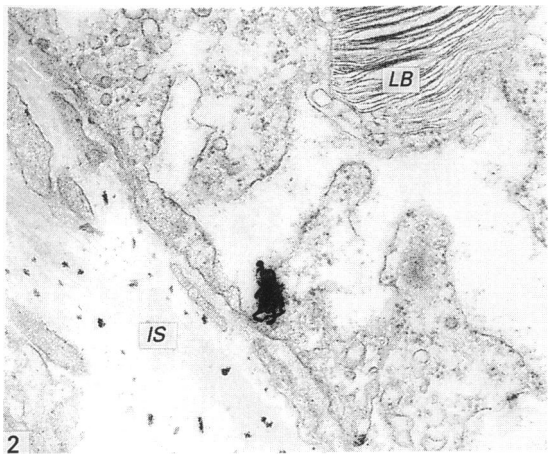

Fig. 1 (*a–c*). Semifine sections of lung tissues 2 minutes after injection of [^{125}I]atrial natriuretic peptides. Silver grains are localised over Type II alveolar epithelial cells (T II arrows, *a*), endothelial cells (*End*, *a*,*b*) and smooth muscle cells of an arteriole (*VSM*, *b*) and a bronchiole (*BSM*, *c*). (*a*) ×1150; (*b*,*c*) ×1700.

Fig. 2. Part of a Type II alveolar cell 2 minutes after injection of [^{125}I]atrial natriuretic peptide. A silver grain is seen on the basal plasma membrane of a Type II alveolar epithelial cell. *IS*, interstitial space; *LB*, lamellar body. ×26000.

Electron microscopy

Type II cells of the control group contained relatively large numbers of lamellar bodies (Fig. 4*a*). At 15 minutes after the injection, lamellar bodies decreased in size and electron-dense multivesicular bodies often appeared in the cytoplasm of the cells (Fig. 4*b*). At 15 and 30 minutes, composite bodies, which contain both electron-dense multivesicular bodies and lamellar structures, were frequently seen in the cells

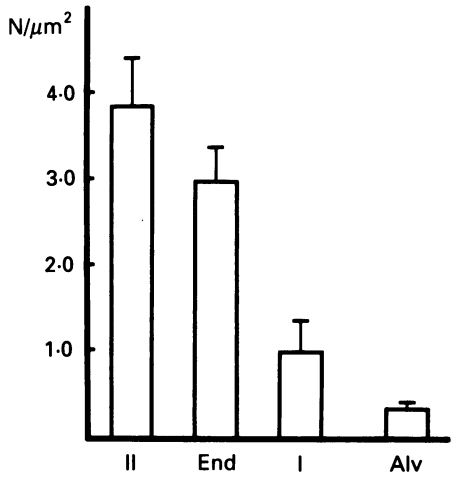

Fig. 3. The numbers of silver grains per unit area of Type II alveolar epithelial cells (II), endothelial cells (End), Type I alveolar epithelial cells (I) and alveolar space (Alv). The numbers of grains in each constituent are significantly higher than the number in the alveolar space ($P < 0{\cdot}01$ by Tukey's comparison test). Vertical bar, ±S.E.

(Fig. 4*c*). At 60 minutes the incidence of larger lamellar bodies increased in the cells, compared with those of other groups (Fig. 4*d*).

Morphometry

RER

Significant increases in the volume and surface densities of RER were detected at 15 minutes; they reached 167% and 143% of the volume and surface densities of the controls (Fig. 5).

Golgi complex

The volume and surface densities of the Golgi complex significantly increased at 5 minutes (Fig. 6). The volume and surface densities peaked at 30 minutes, when they were 315% and 267% of the control values.

Multivesicular bodies

No significant changes were seen in the volume and surface densities of electron-dense multivesicular bodies immediately after the injection of ANP (Fig. 7). However, the densities increased relatively at 15 and 30 minutes compared with the controls.

Lamellar bodies

The volume and surface densities of lamellar bodies significantly decreased at 15 minutes whereas they increased at 60 minutes. The volume and surface densities at 15 minutes decreased to 61·1 and 71·9% of the control values whereas the densities at 60 minutes increased to 157·3 and 135·1% of those at 15 minutes. The numerical density at 60 minutes decreased to 84·4% of the control value (Fig. 8*a*). The mean sphere diameters and individual volumes decreased significantly at 15 and 30 minutes whereas they increased at 60 minutes (Fig. 8*b*). The individual volume at 30 minutes decreased to 71·9% of the control value while at 60 minutes it increased to 121%.

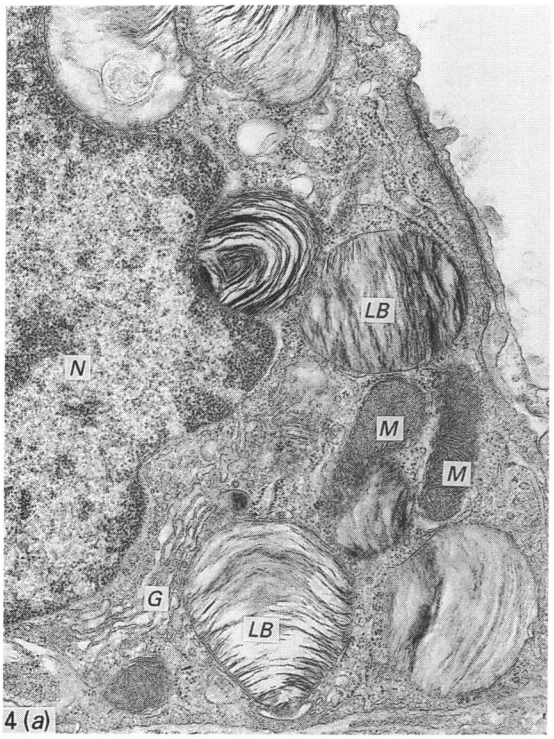

4 (*a*)

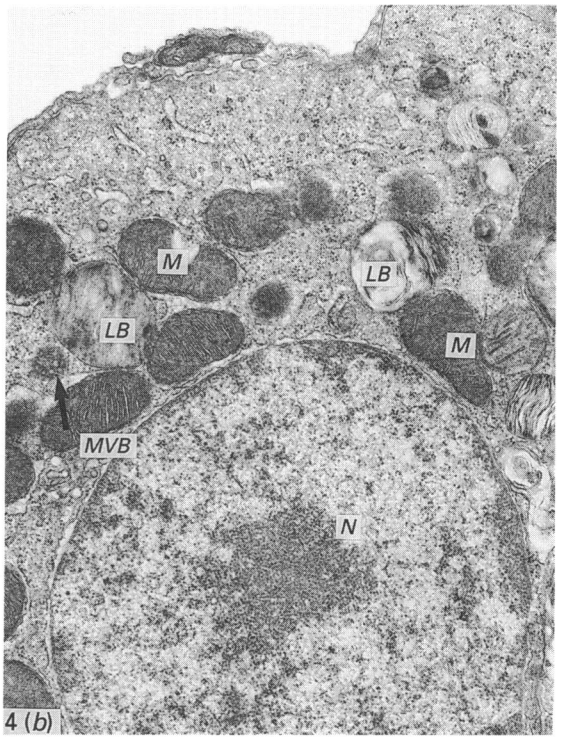

4 (*b*)

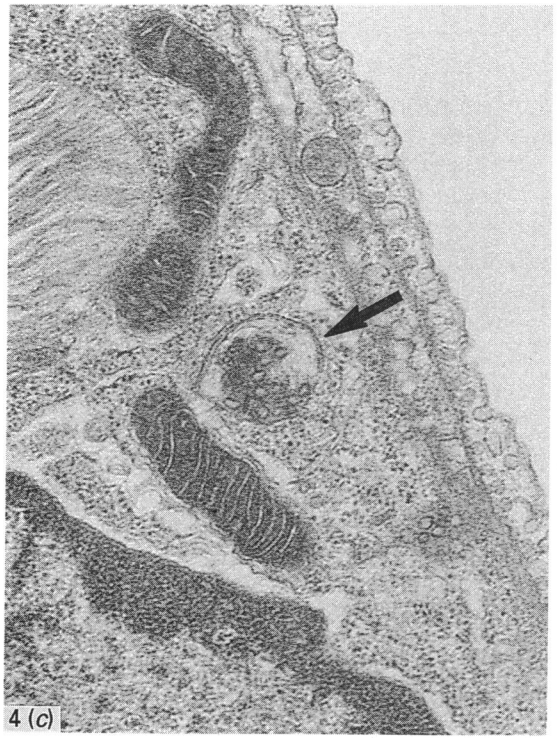

4 (*c*)

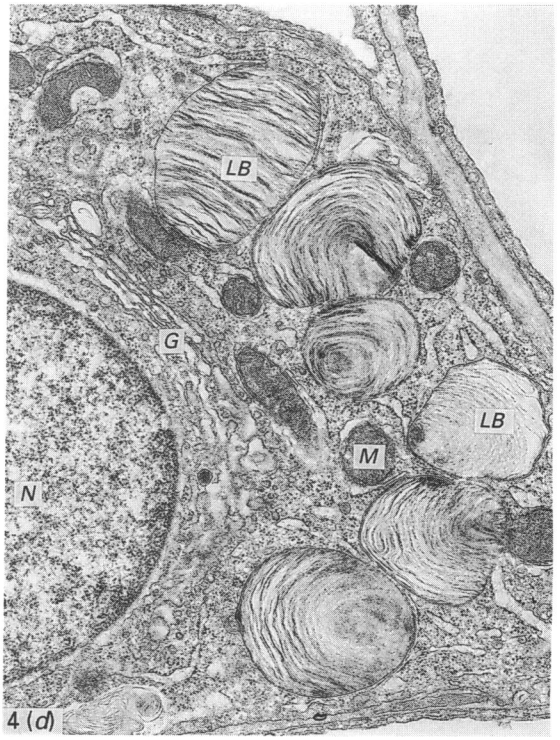

4 (*d*)

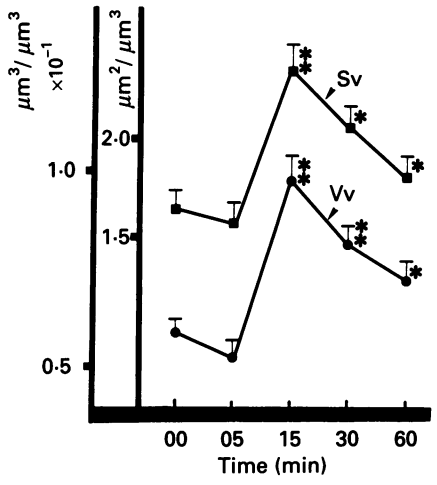

5

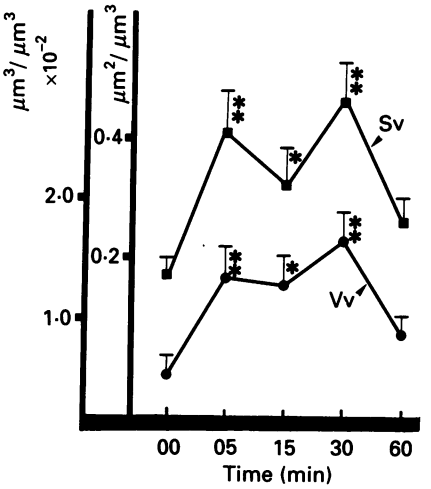

6

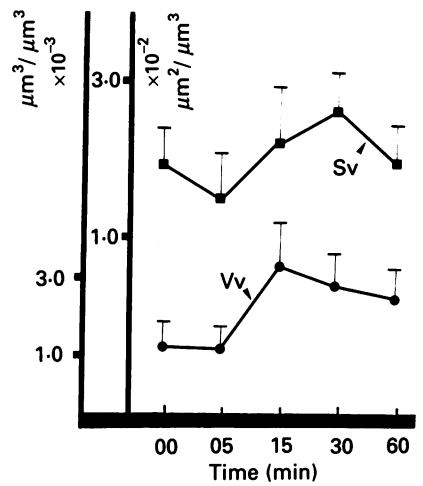

7

Figs. 5–9. Changes in morphometric parameters of various subcellular structures in Type II alveolar epithelial cells after injection of atrial natriuretic peptides. Asterisks indicate the comparison between the controls (0 minutes) and the experimental groups (5, 15, 30, 60 minutes), using Tukey's comparison test: *, $P < 0{\cdot}05$; **, $P < 0{\cdot}01$. Vertical bar, ±S.E.

Fig. 5. The volume (Vv, $\mu m^3/\mu m^3$) and surface (Sv, $\mu m^2/\mu m^3$) densities of rough endoplasmic reticulum. n = 36 at each step.

Fig. 6. The volume and surface densities of the Golgi complex. n = 36 at each step.

Fig. 7. The volume and surface densities of multivesicular bodies. n = 36 at each step.

Fig. 4 (*a–d*). Electron micrographs of Type II alveolar epithelial cells at each stage after injection of atrial natriuretic peptides. (*a*) Before the treatment. Large lamellar bodies (*LB*) are abundantly seen in the cytoplasm of the cell. *G*, Golgi complex; *M*, mitochondria; *N*, nucleus. × 15000. (*b*) At 15 minutes after injection. Larger lamellar bodies disappear from the cytoplasm but several smaller ones can be seen. Multivesicular bodies (*MVB*) often appear in the cytoplasm. × 15000. (*c*) At 30 minutes after injection. A lamellar body possessing a multivesicular body as a constituent, forming a composite body (arrow). These are often discernible at this time. × 37000. (*d*). At 60 minutes after injection. Large lamellar bodies increase again in the cytoplasm. × 15000.

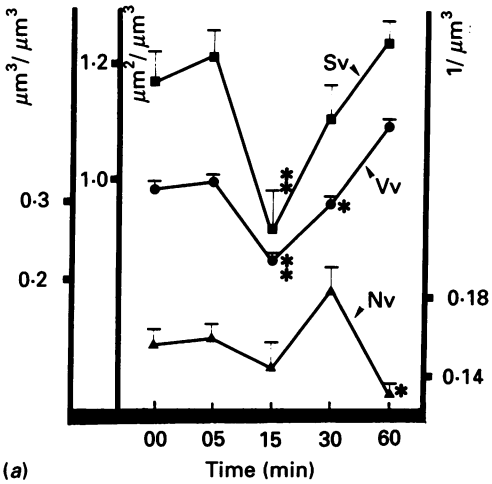

8 (*a*)

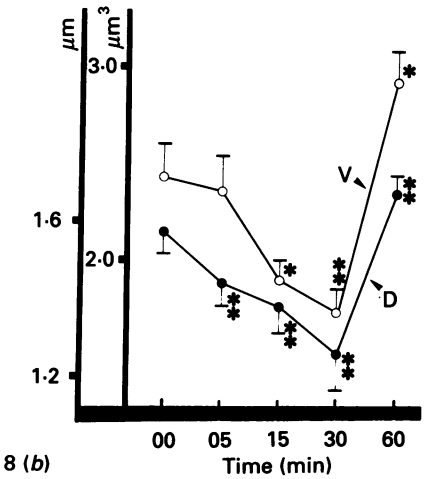

8 (*b*)

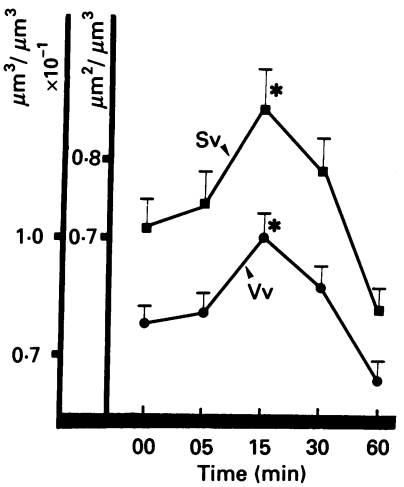

9

Fig. 8 (*a–b*). The volume, surface and numerical (Nv, $1/\mu m^3$) densities of lamellar bodies (*a*), and their individual volumes (V, μm^3) and mean sphere diameters (D, μm) (*b*). The differences in volume and surface densities between 15 and 60 minutes after injection were 57·3% ($P < 0{\cdot}01$) and 35·1% ($P < 0{\cdot}01$), respectively; n = 36 at each step except for the diameters (n = 360).

Fig. 9. The volume and outer surface densities of mitochondria. n = 36 at each step.

Mitochondria

Significant increases were detected in the volume and surface densities of mitochondria at 15 minutes (Fig. 9). The increase in the volume density at 15 minutes was 27·3% while that in the surface density was 21·4%.

DISCUSSION

The uptake of [^{125}I]ANP is significantly inhibited by simultaneous injection of an excess of cold ANP and very few silver grains were detected in the alveolar tissue or in glomeruli of the kidney. This suggests the possibility that the silver grains over the structures after the injection of [^{125}I]ANP alone represent real binding sites.

The present autoradiographic results on the distribution of binding sites of ANP (Leu 99–Tyr 126) in the lung almost agree with previous findings by Bianchi *et al.* (1985) who have used Arg 101–Tyr 126 ANP. In the present study, however, labelling is also detected in Type II cells and smooth muscle cells of bronchi and bronchioles in addition to endothelial cells and smooth muscle cells of vessels. O'Donnell, Garippa & Welton (1985) have shown that ANP induces the relaxation of isolated guinea-pig trachea and pulmonary artery. Therefore, smooth muscle cells of bronchi and bronchioles may possess binding sites for ANP as presented here.

Until recently, no investigation has been reported on cellular changes after the administration of ANP but the present morphometric results demonstrate marked responses of Type II cells. In particular, the RER and Golgi complex increase their volume and surface densities after the injection of ANP. These results suggest that ANP facilitates protein synthesis and intracellular transport of synthesised proteins. In the present study, however, it is paradoxical that the volume and surface densities of the Golgi complex increase prior to the increases in those of the RER. With regard to the peaks of the densities of both organelles, those of the Golgi complex occur after those of the RER. This indicates that protein synthesis and transport of synthesised proteins occur sequentially from the RER to the Golgi complex. Therefore, the increases in the volume and surface densities of the Golgi complex 5 minutes after the injection may not be due to transport of proteins synthesised by the stimulation of ANP.

The present study demonstrates that electron-dense multivesicular bodies increase their volume and surface densities at 15 and 30 minutes, relative to those of the control group. Chevalier & Collet (1972) have shown, using an autoradiographic technique, that the formation of lamellar bodies occurs sequentially from the RER via the Golgi complex, multivesicular bodies and composite bodies to lamellar bodies. Thus, the increases in volume and surface densities of multivesicular bodies at 15 and 30 minutes suggest that Type II cells actively produce lamellar bodies at those times.

With regard to the alterations in lamellar bodies after the injection of ANP, the following results may be important in relation to secretion and formation of lamellar bodies. (1) The volume and surface densities and the individual volumes decrease at 15 minutes, whereas the numerical densities do not change significantly at this time. These results suggest that Type II cells secrete lamellar bodies 15 minutes after the injection. (2) The volume and surface densities begin to increase at 30 minutes, and increase still more at 60 minutes compared to those of the controls, although the individual volume at 30 minutes is smallest. Moreover, the morphometric parameters of the RER, Golgi complex and multivesicular bodies increase in Type II cells prior to the increases in the lamellar bodies. The results suggest that the increases in the volume and surface densities of lamellar bodies at 60 minutes are related to the increases in those of the RER and multivesicular bodies. Therefore, it seems likely that ANP facilitates the formation of lamellar bodies in Type II cells in addition to the production of their secretion.

The present study demonstrates that the volume and surface densities of mitochondria significantly increase 15 minutes after the injection. Mitochondria are known to be a site of energy production. Massaro, Weiss & Simon (1970) have reported that the secretion of macromolecules into the alveolar spaces is an energy-dependent process. From experiments using lung slices of various animals, Massaro, Gail & Massaro (1975) and Massaro & Massaro (1977) have speculated that mitochondrial volume densities in Type II cells change in proportion to oxygen consumption and secretory activity of the cells. In the present study, the significant

increases in volume and surface densities of mitochondria occur simultaneously with the decrease in those of lamellar bodies. This suggests that Type II cells actively secrete surfactant 15 minutes after the injection of ANP. Moreover, the energy supply at 15 minutes may also be necessary for protein synthesis and intracellular transport of synthesised proteins related to the formation of lamellar bodies.

Inomata *et al.* (1987) have reported that ANP prevents pulmonary oedema induced by arachidonic acid treatment in isolated perfused lung from guinea-pig. It is well known that pulmonary oedema induces alveolar collapse which is lessened by pulmonary surfactant. Therefore, our present results concerning the action of ANP on Type II cells are compatible with those on the prevention of pulmonary oedema reported by Inomata *et al.* (1987). The present work, as a whole, suggests that ANP plays an important role in regulation of respiratory conditions in the lung.

SUMMARY

Effects of atrial natriuretic peptides (ANP) on Type II cells of the rat lung were examined, using autoradiographic and morphometric techniques.

The injection of an excess of ANP, together with [^{125}I]ANP, significantly inhibited the uptake of radioactive ANP in the lung tissue. Following autoradiography, silver grains of [^{125}I]ANP labelled Type II cells, endothelial cells and smooth muscle cells of vessels, bronchi and bronchioles. As for morphometric changes in subcellular structures of Type II cells after the injection of ANP, the volume and surface densities of the rough endoplasmic reticulum increased at 15 minutes, while those of the Golgi complex increased from 5 minutes, peaking at 30 minutes. At 15 minutes the volume and surface densities of mitochondria significantly increased. The volume and surface densities of multivesicular bodies with an electron-dense matrix also increased from 15 minutes after the injection. Lamellar bodies showed decreased volume and surface densities at 15 minutes whereas the densities showed an increase at 30 minutes and were higher at 60 minutes than those in the control.

These results suggest that Type II cells provide a binding site for ANP which facilitates the production of lamellar bodies in addition to their secretion.

REFERENCES

Bianchi, C., Gutkowska, J., Thibault, G., Garcia, R., Genest, J. & Cantin, M. (1985). Radioautographic localization of ^{125}I-atrial natriuretic factor (ANF) in rat tissues. *Histochemistry* **82**, 441–452.

Cantin, M., Gutkowska, J., Thibault, G., Milne, R. W., Ledoux, S., Minli, S., Chapeau, C., Garcia, R., Hamet, P. & Genest, J. (1984). Immunocytochemical localization of atrial natriuretic factor in the heart and salivary glands. *Histochemistry* **80**, 113–127.

Chevalier, G. & Collet, A. J. (1972) *In vivo* incorporation of choline-^{3}H, leucine-^{3}H and galactose-^{3}H in alveolar type II pneumocytes in relation to surfactant synthesis. A quantitative radioautographic study in mouse by electron microscopy. *Anatomical Record* **174**, 289–310.

De Bold, A. J., Borenstein, H. B., Veress, A. T. & Sonnenberg, H. (1981). A rapid and potent natriuretic response to intravenous injection of atrial myocardial extract in rats. *Life Sciences* **28**, 89–94.

DeCamara, D. L., Moss, G. S. & Das Gupta, T. K. (1979). Influence of sympathetic nervous system on surfactant production. *Annals of Surgery* **189**, 416–425.

De Lean, A., Racz, K., Gutkowska, J., Nguyen, T.-T., Cantin, M. & Genest, J. (1984). Specific receptor-mediated inhibition by synthetic atrial natriuretic factor of hormone-stimulated steroidogenesis in cultured bovine adrenal cells. *Endocrinology* **115**, 1636–1638.

Dobbs, L. G. & Mason, R. J. (1979). Pulmonary alveolar type II cells isolated from rats. Release of phosphatidylcholine in response to beta-adrenergic stimulation. *Journal of Clinical Investigation* **63**, 378–387.

Farrell, P. M. & Avery, M. E. (1975). Hyaline membrane disease. *American Review of Respiratory Diseases* **111**, 657–688.

Garcia, R., Thibault, G., Cantin, M. & Genest, J. (1984). Effect of a purified atrial natriuretic factor on rat and rabbit vascular strips and vascular beds. *American Journal of Physiology* **247**, R34–R39.

GIGER, H. & RIEDWYL, H. (1970). Bestimmung der Grossenverteilung von Kugeln aus Schnittkreisradien. *Biometrische Zeitschrift* **12**, 156–162.

GOERKE, J. (1974). Lung surfactant. *Biochimica et biophysica acta* **344**, 241–261.

GOLDENBERG, V. E., BUCKINGHAM, S. & SOMMERS, S. C. (1969). Pilocarpine stimulation of granular pneumocyte secretion. *Laboratory Investigation* **20**, 147–158.

GREENWOOD, F. C. & HUNTER, W. M. (1963). The preparation of ^{131}I-labelled human growth hormone of high specific radioactivity. *Biochemical Journal* **89**, 114–122.

INOMATA, N., OHNUMA, N., FURUYA, M., HAYASHI, Y., KANAI, Y., ISHIHARA, T., NOGUCHI, T. & MATSUO, H. (1987). Alpha-human atrial peptide prevents pulmonary edema induced by arachidonic acid treatment in isolated perfused lung from guinea pig. *Japanese Journal of Pharmacology* **44**, 211–214.

ISHIDO, M., FUJITA, T., HAGIWARA, H., SHIMONAKA, M., SAHEKI, T., HIRATA, Y. & HIROSE, S. (1986). Physical and functional association of the atrial natriuretic peptide receptor with particulate guanylate cyclase as demonstrated using detergent extracts of bovine lung membranes. *Biochemical and Biophysical Research Communications* **140**, 101–106.

MASSARO, D., WEISS, H. & SIMON, M. R. (1970). Protein synthesis and secretion by lung. *American Review of Respiratory Diseases* **101**, 198–206.

MASSARO, G. D., GAIL, D. B. & MASSARO, D. (1975). Lung oxygen consumption and mitochondria of alveolar epithelial and endothelial cells. *Journal of Applied Physiology* **38**, 588–592.

MASSARO, G. D. & MASSARO, D. (1977). Mitochondria of the pulmonary granular pneumocyte in different species. *American Review of Respiratory Diseases* **115**, 359–361.

METZ, J., MUTT, V. & FORSSMANN, W. G. (1984). Immunohistochemical localization of cardiodilation in myoendocrine cells of the cardiac atria. *Anatomy and Embryology* **170**, 123–127.

O'DONNELL, M., GARIPPA, R. & WELTON, A. F. (1985). Relaxant activity of atriopeptins in isolated guinea-pig airway and vascular smooth muscle. *Peptides* **6**, 597–601.

OYARZUN, M. J. & CLEMENTS, J. A. (1978). Control of lung surfactant by ventilation, adrenergic mediators, and prostaglandins in the rabbit. *American Review of Respiratory Diseases* **117**, 879–891.

SEIDAH, N. G., LAZURE, C., CHRÉTIEN, M., THIBAULT, G., GARCIA, R., CANTIN, M., GENEST, J., NUTT, R. F., BRADY, S. F., LYLE, T. A., PALEVEDA, W. J., COLTON, C. D. & CICCARONE, T. M. (1984). Amino acid sequence of homologous rat atrial peptides: Natriuretic activity of native and synthetic forms. *Proceedings of the National Academy of Sciences of the U.S.A.* **81**, 2640–2644.

SHIMONAKA, M., SAHEKI, T., HAGIWARA, H., ISHIDO, M., NOGI, A., FUJITA, T., WAKITA, K., INODA, Y., KONDO, J. & HIROSE, S. (1987). Purification of atrial natriuretic peptide receptor from bovine lung. Evidence for a disulfide-linked subunit structure. *Journal of Biological Chemistry* **262**, 5510–5514.

WATANABE, M. & UCHIYAMA, Y. (1988). Twenty-four hour variations in subcellular structures of rat pancreatic islet B-, A- and D-cells, and of portal plasma glucose and insulin levels. *Cell and Tissue Research* **253**, 337–345.

WEIBEL, E. R. (1979). *Stereological Methods. Practical Methods for Biological Morphometry.* New York: Academic Press.

WU, B., KIKKAWA, Y., ORZALESI, M. M., MOTOYAMA, E. K., KAIBARA, M., ZIGAS, C. J. & COOK, C. D. (1973). The effect of thyroxine on the maturation of fetal rabbit lungs. *Biology of the Neonate* **22**, 161–168.